Development Genes and Evolution
https://doi.org/10.1007/s00427-020-00645-w

ORIGINAL ARTICLE

Notch signaling patterns head horn shape in the bull-headed dung beetle *Onthophagus taurus*

Jordan R. Crabtree[1] · Anna L. M. Macagno[1] · Armin P. Moczek[1] · Patrick T. Rohner[1] · Yonggang Hu[1]

Received: 31 July 2019 / Accepted: 14 January 2020

Abstract

Size and shape constitute fundamental aspects in the description of morphology. Yet while the developmental-genetic underpinnings of trait size, in particular with regard to scaling relationships, are increasingly well understood, those of shape remain largely elusive. Here we investigate the potential function of the Notch signaling pathway in instructing the shape of beetle horns, a highly diversified and evolutionarily novel morphological structure. We focused on the bull-headed dung beetle *Onthophagus taurus* due to the wide range of horn sizes and shapes present among males in this species, in order to assess the potential function of Notch signaling in the specification of horn shape alongside the regulation of shape changes with allometry. Using RNA interference-mediated transcript depletion of *Notch* and its ligands, we document a highly conserved role of Notch signaling in general appendage formation. By integrating our functional genetic approach with a geometric morphometric analysis, we find that Notch signaling moderately but consistently affects horn shape, and does so differently for the horns of minor, intermediate-sized, and major males. Our results suggest that the function of Notch signaling during head horn formation may vary in a complex manner across male morphs, and highlights the power of integrating functional genetic and geometric morphometric approaches in analyzing subtle but nevertheless biologically important phenotypes in the face of significant allometric variation.

Keywords Size · Allometry · *Serrate* · Appendage · Geometric morphometrics · Polyphenism

Introduction

Size and shape constitute fundamental aspects in the description of morphology (Mitteroecker et al. 2013). Evolutionary changes in the relative sizes and shapes of traits are credited with facilitating much of the organismal diversity present today (Thompson 1917; Huxley 1932; Casasa and Moczek 2019). Yet while the quantitative and developmental-genetic underpinnings of trait size are increasingly well understood (Pan 2007; Koyama et al. 2013; Nijhout et al. 2014; Gokhale and Shingleton 2015), those of shape variation, in particular of novel complex traits, remain largely unexplored, due at least in part to methodological challenges. Unlike differences in size, which can be expressed with rather simple univariate data (e.g., length, width, area, etc.), the complex characteristics of shape, and its dependence on overall size, require a multivariate analytical approach (Klingenberg 2016; Prpic and Posnien 2016; Outomuro and Johansson 2017). Geometric morphometrics provide powerful tools to target these aspects of morphology in the context of the developmental evolution of novel complex traits.

Many scarab beetles possess rigid projections of the exoskeleton collectively referred to as horns. These structures fulfill even the most stringent definition of evolutionary novelty, being "neither homologous to any body part in the ancestral lineage nor serially homologous to any other body part of the same organism" (Müller and Wagner 1991). Phylogenetic reconstructions of horn evolution reveal multiple gains, losses, and regains, alongside rapid diversification of horn shape (Emlen et al. 2005b, 2007). The vast diversity of horn morphologies seen today reflects this evolutionary history, and horn locations, sizes, and shapes can vary extensively even between closely related species. In

Communicated by Nico Posnien

Electronic supplementary material The online version of this article (https://doi.org/10.1007/s00427-020-00645-w) contains supplementary material, which is available to authorized users.

✉ Yonggang Hu
yohu@iu.edu

[1] Department of Biology, Indiana University, Bloomington, IN 47405, USA

Published online: 20 January 2020

the tribe Onthophagini, where these structures have been particularly well studied, horns positioned posteriorly on the head are prevalent (Emlen et al. 2005a), and include diverse shapes such as single, paired, forked, or branched (Fig. 1). While horn morphology differs strongly even among closely related species, horn shape also shows strong developmental plasticity within species, such as in the transition from relatively straight to curved horns in the polyphenic *Onthophagus taurus* (Fig. 1).

In the majority of horned beetle species described to date, horn expression is confined to males and has been traditionally characterized by the scaling relationship between body size and horn size. Scaling is typically non-linear, with larger body sizes resulting in disproportionately larger head horns, and distinct morphs existing within the same species (Emlen et al. 2006; Moczek and Rose 2009; Kijimoto and Moczek 2016). Subtle changes in horn/body size scaling are considered important drivers in the great diversification of beetle horns (Tomkins et al. 2005; Kodric-Brown et al. 2006; Emlen et al. 2007). Yet, a simple measurement of horn size is insufficient to capture the complexity of horn morphology and potential changes therein with body size (Simmons and Fitzpatrick 2016), a challenge that necessitates the use of more complex multivariate methods. At the same time, extant diversity in the sizes and shapes of beetle horns may not be surprising given their function as weapons to battle rival males over reproductive access to females (O'Brien et al. 2018). Previous studies have established a link between horn shape and its precise function within the context of a species-specific fighting style, suggesting that male–male competition plays

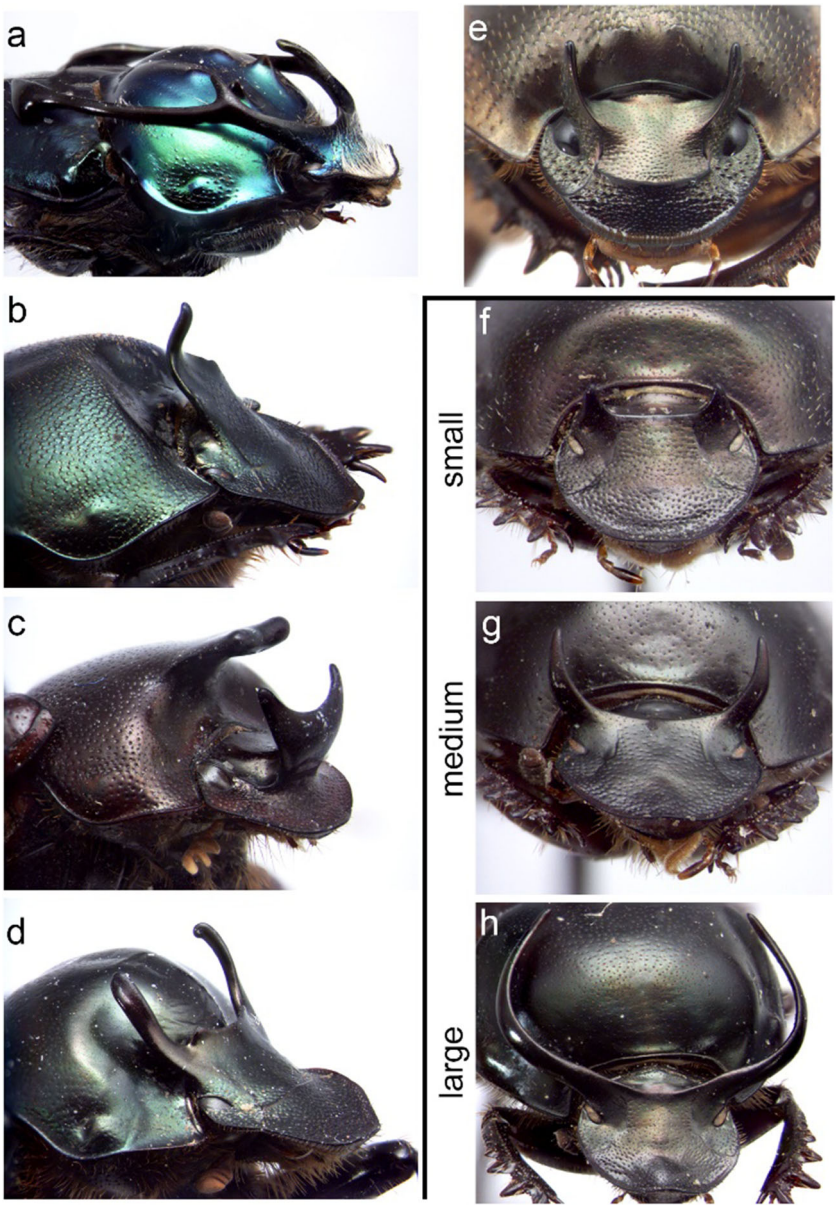

Fig. 1 Morphological diversity of head horns in the tribe Onthophagini. **a**–**h** Typical shape variation of the head horn in closely related beetle species: branched horn in *Proagoderus rangifer* (**a**), single horn in *Onthophagus medius* (**b**), forked horn in *O. lunatus* (**c**), and paired horn in *O. australis* (**d**), *Digitonthophagus gazella* (**e**), and *O. taurus* (**f**–**h**). **f**–**h** The change in size and shape (especially curvature) of the paired head horns in small (**f**), medium (**g**), and large (**h**) male *O. taurus*

an important role in horn shape diversification (McCullough et al. 2014). However, while the ultimate (i.e., selective) drivers of horn shape variation are becoming increasingly well understood, the proximate developmental mechanisms that underlie or bias the evolution of horn shape remain largely unknown.

Here we sought to investigate the potential function of the Notch signaling pathway in the regulation of horn shape in the bull-headed dung beetle *O. taurus*. The Notch signaling pathway plays a well-documented role in the regulation of traditional appendages such as legs, mouthparts, and antennae, including the formation and positioning of joints, in particular through the short-range regulation of cellular proliferation, orientation, and apoptosis (Kojima 2004, 2017). The pathway consists of a membrane-bound receptor Notch (N), and two main receptor ligands Delta (Dl) and Serrate (Ser). We focused on this pathway because (1) even though horns do not contain joints, cell death and reorientation have been documented during the re-patterning of head horn shape during the pupal stage (Kijimoto et al. 2010), (2) previous transcriptomic screens detected the expression of Notch pathway members during dorsal head formation (Kijimoto et al. 2009; Choi et al. 2010), and (3) previous studies have implicated other appendage patterning pathways in the formation of beetle horns (Moczek and Rose 2009; Wasik and Moczek 2011; Kijimoto and Moczek 2016). We focused on *O. taurus* to study the developmental underpinnings of horn shape due to the pronounced nutrition-sensitive developmental plasticity of male horn morphology. In this species, the strong sigmoidal scaling relationship between horn length and body size results in small (minor) males expressing very short and relatively straight head horns, whereas large (major) males harbor approximately 10-fold longer, curved, and slightly twisted horns (Fig. 1), with relatively few intermediates existing in natural populations (Moczek and Emlen 1999). This affords us the opportunity to assess the potential function of Notch signaling not just in the general specification of horn shape, but also in the regulation of shape changes with size.

Using RNA interference-mediated transcript depletion of *N* and its ligands, we begin by documenting the role of Notch signaling in general appendage formation. By integrating our functional genetic analysis with a geometric morphometric analysis of horn shape, we next document a strong covariation between horn size and shape, and then assess the role of Notch signaling in the regulation of horn shape while controlling for overall size in different morphs. Finally, we discuss the implications of our findings in our understanding of the developmental evolution of horn shape in general, and the change in horn shape with size in particular.

Materials and methods

Animal husbandry

Onthophagus taurus adults were collected courtesy of John Allen from Paterson Farm near Ravenswood, Western Australia, in 2018. Beetles were maintained as laboratory colonies at 24 °C in Bloomington, Indiana, under a 16:8 h light:dark cycle and reared as described previously (Kijimoto et al. 2009; Choi et al. 2010).

Identification of candidate genes and DNA fragment synthesis

The amino acid sequences of *Notch*, *serrate*, and *delta* of *Tribolium castaneum* were used as queries to execute blast searches against the *O. taurus* genome and transcriptome (https://i5k.nal.usda.gov/webapp/blast/). Best hits were confirmed using reciprocal blasts. Corresponding DNA sequences were retrieved from the transcriptomes, and partial fragments of the coding DNA sequence were synthesized by gBlocks Gene Fragment (Integrated DNA Technologies, USA).

dsRNA synthesis and injection

We followed the protocol of dsRNA synthesis and injection described previously (Linz et al., 2019). In brief, T7 promoter sequences were added to both ends of the templates for in vitro transcript by PCR via gene-specific primers along with a T7 promoter sequence at the 5′ end (see Table S1 for primer sequences). dsRNA was synthesized with MEGAscript T7 transcription kit (Invitrogen, USA), then purified using MEGAclear kit (Invitrogen, USA). Finally, generated dsRNA was eluted with nuclease-free water, and the concentration was measured using Nanodrop 1000 (Thermo Scientific, USA). The offspring of laboratory colonies were used as a source of larvae for injection. First- and second instar larvae were transferred from their natal brood ball into 12-well plates containing artificial brood balls (as described in Shafiei et al., 2001) and monitored until they molted into the third larval instar (L3). dsRNA injection was carried out at the early stage of L3 (see Table 1 for injection details). The same volume of injection buffer was injected at the same developmental stage to generate negative control individuals. Phenotypes were observed and recorded at pupal and adult stages, respectively. Phenotypic penetrance was calculated as: $\frac{\text{number of pupae showing the phenotype}}{\text{total number of pupated individuals}} \times 100\%$.

Tissue dissection and in situ hybridization chain reaction

Onthophagus taurus individuals at the prepupal stage were selected for sample preparation. The whole head was

Table 1 Summary of dsRNA injections of *Notch*, *serrate*, and *delta*

dsRNA	Concentration (μg/μl)	Injected number	Pupated number	Eclosed to adult	Phenotypic penetrance
Notch	1.0	10	1	1	100%
	0.5	24	2	0	
	0.25	32	2	0	
	0.1	29	0	0	
serrate	1.0	6	2	1	100%
	0.8	24	6	2	
	0.7	11	9	6	
	0.5	356	143	61	
	0.4	18	14	2	
	0.3	54	17	3	
Delta	1.0	6	0	0	0%
	0.5	51	4	1	
	0.25	70	6	4	
	0.1	18	4	0	
	0.05	5	3	0	
	0.025	29	6	5	

dissected and then fixed in 3.7% formaldehyde (FA) solution for 40 min at room temperature. The developing pupal head was dissected out of the larval cuticle in PBS with 0.05% Triton-X (PBT). The genitalia were also dissected in PBT and fixed in 3.7% FA for 15 min at room temperature. After several washes with PBT, both head and genitalia were dehydrated through 30%, 70%, and 100% methanol series in PBT. The samples were kept in 100% methanol for at least 1 h at − 20 °C, rehydrated through 70%, 30% methanol series in PBT, and rinsed several times in PBT. Following that, tissues were subjected to a 5-min proteinase K (10 μg/μl) digestion, then rinsed several times in PBT. After the postfixation in 3.7% FA for 20 min and several washes in PBT, the samples were subsequently processed using standard procedures of in situ hybridization chain reaction (in situ HCR v3.0 protocol for sample in solution) (Choi et al. 2018). DAPI counterstain was also applied to tissues to mark the nucleus. After several washes in PBT, tissues were mounted on slide with Prolong glass antifade mountant (Invitrogen, USA), then observed and photographed on an imager Z2 microscope (Zeiss, Germany).

Geometric morphometrics

We sought to determine the effect of *ser* knockdown on the shape of head horns in different male morphs by contrasting ser^{RNAi} males to buffer-injected (control) males (major: 18 ser^{RNAi}, 23 control; minor: 11 ser^{RNAi}, 28 control; intermediate: 5 ser^{RNAi}, 16 control). Only ser^{RNAi} individuals that presented clear knockdown phenotypes in anatomical areas other than the head were included in the analysis. Because downregulation of *ser* affected thoracic width (Fig. 2k and i), i.e., the usual proxy for body size in *O. taurus* (Macagno et al. 2018), morphs could not be defined on the basis of the scaling relationship between horn length and body size as in previous studies (e.g., Casasa and Moczek 2018). Instead, males were identified as major, minor, or intermediate based on whether horns were longer, shorter, or approximately equal to the distance between horns, respectively.

We took calibrated images of horns with 2D image acquisition equipment including a stereoscope (Leica MZ-16, USA), a digital camera (Scion, USA), and ImageJ (Schneider et al. 2012). We ensured flat horizontal positioning of the horns by setting optics for a very shallow depth of field and placing the whole perimeter of the horn in the same focal plane. We then used geometric morphometrics (Bookstein 1991; Adams et al. 2004) and the method of sliding semilandmarks (Zelditch et al. 2004; Mitteroecker and Gunz 2009; Goczał et al. 2019) to quantify variation in horn size and shape. The paired head horns of *O. taurus* are bilaterally symmetrical, and since quantifying asymmetric variation was not an aim of this study, analyses were performed only on one side—the right horn (Adams 2004; Head and Polly 2015; Macagno et al. 2016; Romiti et al. 2017; Rohner et al. 2019). Using tpsDig2w32 (version 2.31) (Rohlf, 2018a) and tpsUtil32 (version 1.76) (Rohlf, 2018b), we digitized four anatomically distinct locations that could be identified reliably in all specimens as fixed landmarks (1, 2, 16, and 30), and defined the curvature of the horns with evenly spaced semilandmarks (3–15 and 17–29) (Fig. 5). We tested the tangent space approximation in tpsSmallw32 (version 1.34) (Rohlf, 2017b). In tpsRelw32 (version 1.69) (Rohlf, 2017a), we first superimposed the data and slid the semilandmarks (Rohlf, 2015), and then saved the centroid size (a shape-independent estimate of horn size: Klingenberg, 2016) and

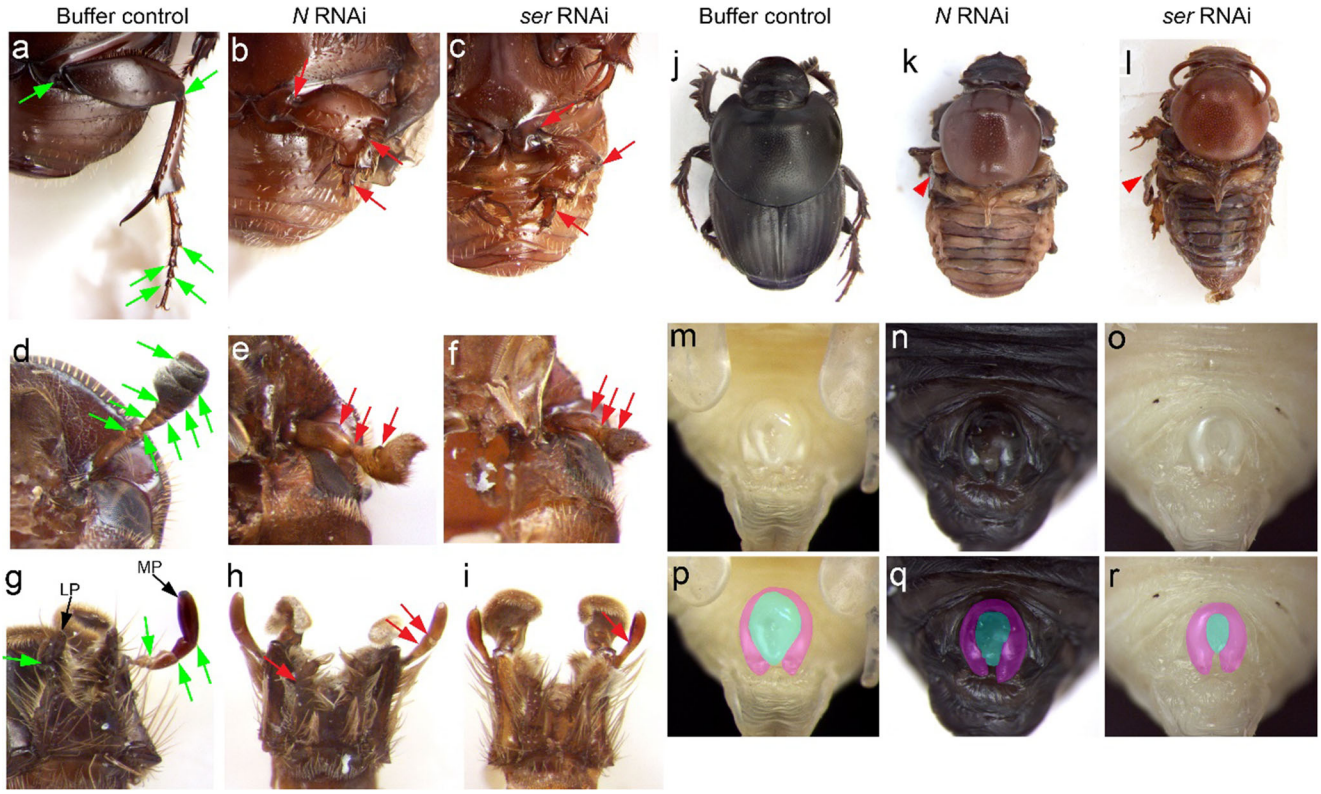

Fig. 2 Appendage defects following RNAi targeting Notch signaling genes. **a**–**i** Both N^{RNAi} and ser^{RNAi} similarly induced a reduction in length and loss of joints between segments of legs (**b**, **c**), antennae (**e**, **f**), maxillary palps, and labial palps (**h**, **i**). Green arrows indicate joints between appendage segments in buffer control individuals (**a**, **d**, **g**), while red arrows highlight defects in RNAi individuals (**b**, **c**, **e**, **f**, **h**, **i**). **j**–**l** Both also strongly reduced or eliminated wings (indicated by red arrowhead). **m**–**r** N^{RNAi} and ser^{RNAi} reduced or deleted the central area of the male genitalia, externally visible during the pupal stage. MP, maxillary palp; LP, labial palp

the aligned (=Procrustes-transformed) coordinates of each specimen. Both sets of variables were then imported into R 3.5.2 (R Core Team 2018) for subsequent analyses.

We first performed a principal component analysis (PCA) of horn shape variables to illustrate the overall variation in shape, and its covariation with size, using the plotTangentSpace() function as implemented in the R-package geomorph 3.1.2 (Adams et al. 2019). We then modeled horn shape (i.e., the set of Procrustes-transformed coordinates) as a function of log-transformed centroid size (log(cs)), treatment (Ctrl vs ser^{RNAi}), morph (minor, major, intermediate), and all their interactions using a Procrustes ANOVA (Goodall 1991) as implemented in the function procD.lm(). This is a distance-based ANOVA technique that uses permutation tests to assess the effect of predictor variables. All significance testing was done with the randomized residual permutation procedure (RRPP) implemented in the geomorph library (Collyer and Adams 2018, 2019). Because both the effect of allometry and of *ser* knockdown on horn shape depended on morph (significant two-way interactions with log(cs) and treatment: Table 2), it was difficult to illustrate and analyze the effect of treatment independent of allometric variation within morphs. To better understand the effects of allometry and of *ser* knockdown, we hence assessed the effect of log(cs), treatment and their interaction on horn shape within each morph, with Procrustes ANOVAs as detailed above.

Pronounced allometric variation (i.e., the dependence of horn shape on its size) may mask or confound shape differences between treatments due to differences in scaling caused by the treatment, or due to differences in the size composition of the samples (Mitteroecker et al. 2004). Here, we sought to control for allometric variation within morphs by first regressing the Procrustes-transformed coordinates onto log(cs) using procD.lm(), and then using only the residual shape information for further analysis (Klingenberg 2016). This approach requires a common allometry in all groups, and was therefore used in the morphs where allometry was not affected by treatment (i.e., minor and major males: significant main effect of treatment, non-significant interaction between log(cs) and treatment; Table 2). To inspect the deformation caused by ser^{RNAi}, we employed the procD.lm() function to model the allometry-adjusted horn shape coordinates as a function of treatment in each morph, then extracted the vectors of shape deformation corresponding to Ctrl and ser^{RNAi} individuals, and visualized the deformation grids using the function plotRefToTarget() in geomorph. Additionally, we ran a PCA and a discriminant analysis with cross-validation on

Table 2 (a) Effect of log(cs) (horn centroid size, log-transformed), treatment (Crtl vs *ser*^{RNAi}), and morph on horn shape, as assessed with a Procrustes ANOVA. The same analysis was repeated within minor (b), intermediate (c), and major males (d)

	Df	SS	r^2	F	Z	P	
a. All males							
log(cs)	1	9.425	0.88	3079.01	3.65	0.001	**
Treatment	1	0.048	< 0.01	15.64	1.82	0.028	*
Morph	2	0.673	0.06	109.86	4.88	0.001	**
log(cs):treatment	1	0.017	< 0.01	5.60	1.78	0.033	*
log(cs):morph	2	0.232	0.02	37.82	5.66	0.001	**
Treatment:morph	2	0.015	< 0.01	2.52	2.26	0.006	**
log(cs):treatment:morph	2	0.005	< 0.01	0.84	0.12	0.450	NS
Residuals	89	0.272	0.03				
Total	100	10.687					
b. Minor males							
log(cs)	1	0.229	0.49	44.92	3.42	0.001	**
Treatment	1	0.056	0.12	11.09	3.17	0.001	**
log(cs):treatment	1	0.003	< 0.01	0.51	0.59	0.729	NS
Residuals	35	0.178	0.38				
Total	38	0.466					
c. Intermediate males							
log(cs)	1	0.147	0.64	56.87	3.02	0.001	**
Treatment	1	0.033	0.14	12.74	3.06	0.002	**
log(cs):treatment	1	0.006	0.03	2.43	1.72	0.041	*
Residuals	17	0.044	0.19				
Total	20	0.230					
d. Major males							
log(cs)	1	0.043	0.34	31.88	3.40	0.001	**
Treatment	1	0.031	0.25	23.14	3.74	0.001	**
log(cs):treatment	1	0.001	0.01	0.97	0.41	0.352	NS
Residuals	37	0.050	0.40				
Total	40	0.127					

"*, $P \leq 0.05$; **, $P \leq 0.01$, NS, not significant

allometry-adjusted shape coordinates of Ctrl and *ser*^{RNAi} individuals, using the function CVA() in the R library Morpho 2.7 (Schlager 2017). We expressed the magnitude of shape difference between treatment groups by means of Procrustes distances, and assessed their significance with permutation tests (10,000 permutation rounds).

In contrast to major and minor males, *ser* knockdown did appear to affect the horn shape allometry of intermediate males (significant interaction between log(cs) and treatment: Table 2). To assess the strength of this effect, we modeled the horn Procrustes-transformed coordinates as a function of log(cs) using procD.lm() separately in Ctrl and *ser*^{RNAi} individuals, extracted the corresponding allometric vectors, and visualized the deformations corresponding to a 0.2 increase of log(cs) compared with the mean shape of each treatment group, using the function plotRefToTarget() in geomorph. To further quantify the similarity between the allometry of Ctrl and *ser*^{RNAi} individuals, we calculated vector correlations between the respective allometric vectors as: $r_{Ctrl,ser^{RNAi}} = \frac{\left|v_{\mathrm{Ctrl}} \cdot v_{ser^{RNAi}}\right|}{\|v_{\mathrm{Ctrl}}\| \times \left\|v_{ser^{RNAi}}\right\|}$. That is, we scaled the dot product of the two allometric vectors by their norm (Pitchers et al. 2013; Testa and Dworkin 2016; Schäfer et al. 2018). We detected small angles and very high correlation between the allometric vectors of Ctrl and *ser*^{RNAi} individuals (detailed in "Results"). In light of this strong congruence and of the small sample size in the *ser*^{RNAi} group ($n = 5$) due to lethality of the dsRNA injection, we interpreted these differences as biologically negligible (as advised in Klingenberg 2016), and proceeded with analyses as previously done in minor and major males, assuming a common allometric slope in the two treatments and adjusting for allometric variation accordingly.

Results

Functional significance of the Notch signaling pathway for general appendage development

Across arthropods, Notch signaling is required for the elongation of appendage discs and joint formation later in development (de Celis et al. 1998; Rauskolb and Irvine 1999; Bishop et al. 1999; Prpic and Damen 2009; Mito et al. 2011; Angelini et al. 2012; Liu 2013). We first assessed the role of Notch signaling during appendage formation in *O. taurus* through RNAi-mediated transcript depletion of *Notch* itself. Of 95

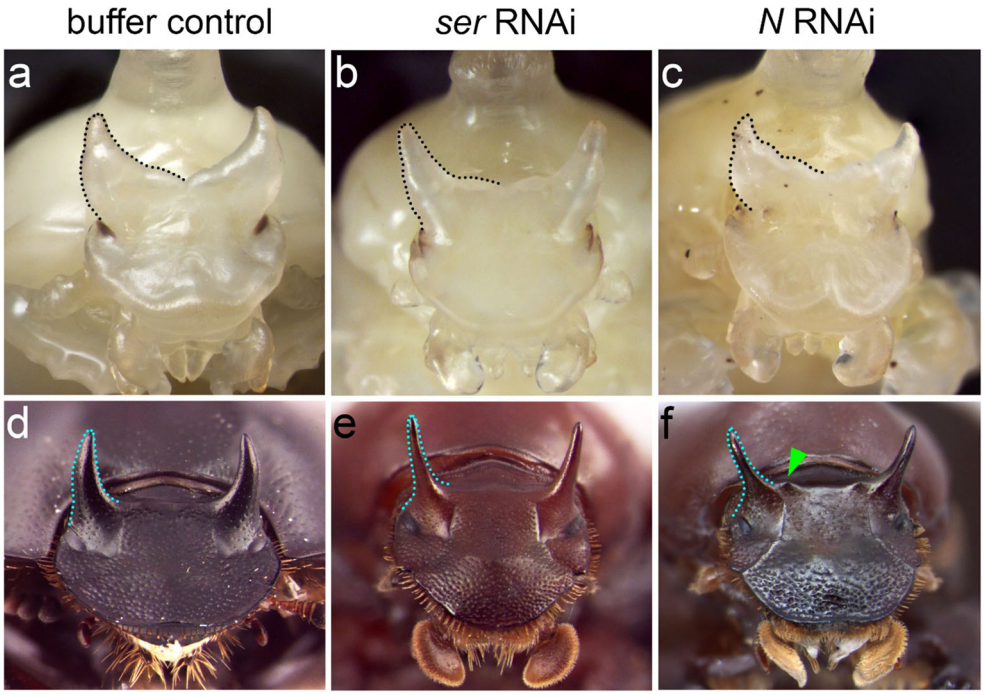

Fig. 3 Head horn phenotypes following RNAi targeting Notch signaling genes. **a**, **d** Control treatments with buffer injection were indistinguishable from untreated beetles. **b**, **e** ser^{RNAi} resulted in less curved, slender horns in pupae (**b**) and adults (**e**). **c**, **f** Knockdown of *N* resulted in similar phenotypes compared to ser^{RNAi} (**b**, **e**). In addition, N^{RNAi} induced a pair of small, pointy cuticular bumps medial to each horn in the adult (green arrowhead in **f**). Black (**a**–**c**) and cyan dotted line (**d**–**f**) highlight the outline of head horns at the pupal and adult stage, respectively

injected animals, only 5 (5.3%) successfully pupated and 1 (1.1%) survived to the adult (Table 1). Despite this low survival rate, all pupae and adult showed consistent phenotypes. N^{RNAi} resulted in the reduction in the length of the entire leg and elimination of leg joints (red arrow in Fig. 2b). Antennae and mouthparts exhibited a similar shortening in length, as well as a loss of joints, and corresponding fusion of segments (Fig. 2d–i). These phenotypes closely resemble those documented across diverse arthropods in previous studies (de Celis et al. 1998; Prpic and Damen 2009; Mito et al. 2011; Angelini et al. 2012; Liu 2013). Further, N^{RNAi} induced severe defects in the lateral margin of the first thoracic segment as well as a strong reduction in the size of wings in both the second and third thoracic segments (Fig. 2k), consistent with the hypothesis of serial homology between the prothoracic lateral margin and bona fide wings (Clark-Hachtel et al. 2013). In addition, we were able to document a defect during genitalia formation in males, resulting in a nearly complete deletion of the central region of the male copulatory organ visible externally during the pupal stage (Fig. 2n, q). Based on our observations, this region contributes to the formation of the endophallus, a membranous distal component of the adult male copulatory organ.

Subsequent knockdowns targeted the *Notch* ligands *ser* and *dl* to determine which ligand may mediate Notch signaling during appendage patterning. dl^{RNAi} resulted in very high mortality even at very low concentrations of injected dsRNA (0.025 μg/μl). In total, of 179 injected animals, most died at the prepupal stage, only 23 (12.8%) successfully pupated and only 10 (5.6%) eclosed as adults (Table 1). However, none of these surviving adults exhibited obvious appendages and horns related defects. In contrast, ser^{RNAi} resulted in comparably moderate mortality (40.7% (191/469) pupation rate, and 16.0% (75/469) eclosion rate) and surviving individuals exhibited knockdown phenotypes in legs, wings, and genitalia similar to those observed following N^{RNAi} (Fig. 2). Copulatory structure dissection confirmed the reduction in size of the male endophallus following ser^{RNAi} (Fig. S1). Collectively, these results document the conserved function of Notch signaling during appendage growth and joint development in *O. taurus* and suggest that the patterning of these traits is mediated at least partly via the ligand *ser*.

Notch signaling and the patterning of the dorsal head

Previous work has shown that the limb gap genes, *hth*, *dac*, and *Dll*, were differentially recruited during the developmental evolution of beetle horns across *Onthophagus* species and sexes (Moczek et al. 2006; Moczek and Rose 2009). Since Notch signaling carries out critical functions during arthropod appendage formation, we sought to determine whether Notch signaling is also similarly significant during the patterning of beetle horns.

To test this hypothesis, we assessed horn phenotypes following larval RNAi against *N* and *ser*. N^{RNAi} moderately affected the shape of pupal head horns, which became more pronounced in the adult stage, resulting in narrower and straighter head horns in intermediate-sized males (Fig. 3c, f). In addition, one pair of tiny cuticular bumps formed ectopically between head horns (green arrow in Fig. 3f), and a subtle shape change was also observable in the corresponding region at the pupal stage (Fig. 3c). Due to the high mortality of N^{RNAi}, we then turned to assess the function of its ligand

ser. We found that the phenotypes induced by ser^{RNAi} paralleled those induced by N^{RNAi} except for the formation of ectopic bumps (Fig. 3b, e).

In addition, knocking down either *N* or *ser* eliminated the outer margin of the dorsal head, leading to bristles normally hidden under the dorsal head becoming more visible from a dorsal view (Fig. 3d–f). Previous studies in *D. melanogaster* revealed that Notch signaling is required for dorsal/ventral (D/V) axis patterning in imaginal discs (de Celis et al. 1996; Domínguez and de Celis 1998), and our results suggest that Notch signaling might function similarly during adult head formation by delineating the boundary separating dorsal from ventral head regions.

The expression pattern of *ser* in pupal head and genitalia primordia

Previous EST and microarray studies revealed the expression of Notch signaling components in the developing head horn (Kijimoto et al. 2009; Choi et al. 2010). However, these expression profiles were detected by isolating total mRNA of the entire horn, thus providing no further information regarding the spatial expression pattern of Notch signaling in the head horn or adjacent head regions. In order to better understand how Notch signaling regulates head horn formation and to distinguish direct and indirect effects of RNAi, we performed whole mount in situ hybridization chain reaction to detect the expression pattern of *ser* during pupal head formation. We replicated this approach for male genitalia. We found *ser* is strongly expressed along the outer margin of the dorsal head and moderately expressed in compound eyes (Fig. 4a–c). The expression pattern of several discrete rings was observed in the presumed antennal joints (Fig. 4a–c). Interestingly, we also found that *ser* expression resembling a semi-circular stripe surrounded the head horn primordia (Fig. 4a, c). Here, *ser* expression was visible beginning with lateral aspects of the horn, passing around posterior horn regions, and extending slightly toward the medial region between horns (Fig. 4a, c). In the male genitalia primordium, *ser* expression was restricted to the central region (i.e., the presumed endophallus) (Fig. 4d–f). Collectively, the expression pattern of *ser* appears to closely parallel the physical locations of ser^{RNAi} phenotypes, and by extension suggests that the ser^{RNAi} phenotypes reported here reflect direct consequences of the downregulation of Notch signaling components rather than potential off-target or indirect effects.

Notch signaling mediates head horn shape in a morph-dependent fashion

In order to assess the effect of Notch signaling on horn shape across the range of horn sizes present within natural populations of this species, we preliminarily performed a PCA of Procrustes-transformed horn shape coordinates. The first principal component alone accounted for over 93% of the overall shape variance, and was tightly correlated with log-transformed centroid size (log(cs)) (Spearman's rho 0.97, two-tailed $P < 0.001$), indicating a substantial contribution of allometry to horn shape variation (Fig. 5). For subsequent analyses, males were identified as major, minor, or intermediate as detailed in the "Methods". Visual

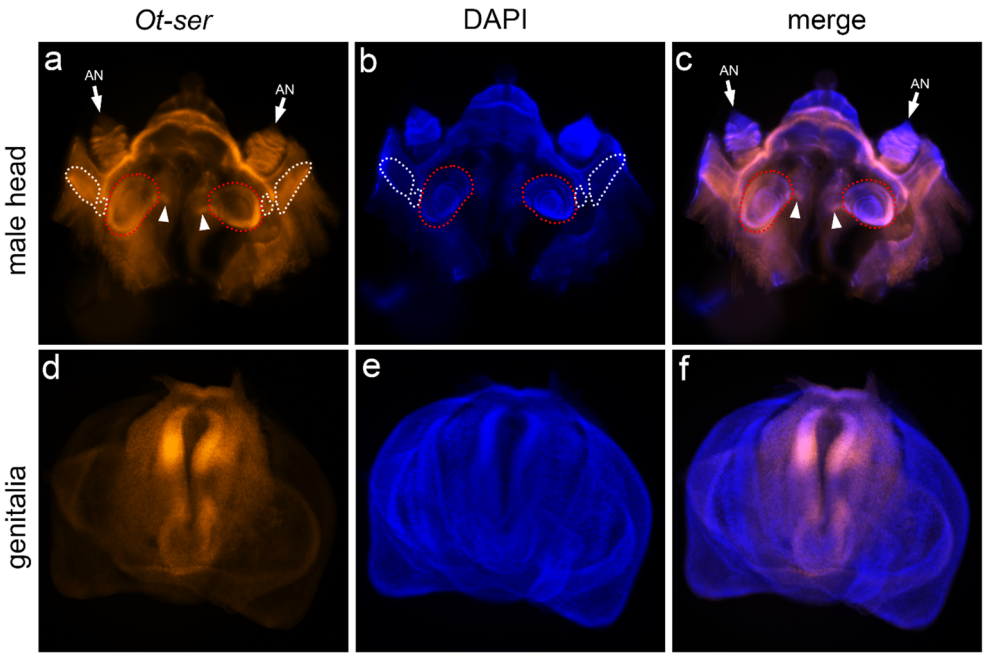

Fig. 4 Expression pattern of *ser* in the developing pupal head and genitalia. **a**–**b** Head primordium stained with *ser* antisense riboprobes and counterstained with DAPI. **c** Combination of **a** and **b**. Arrowheads indicate expression of *ser* in the medial head adjacent to horn primordia (outlined with red dotted line). White dotted lines denote compound eyes. **d**–**f** The same staining in the genital primordium. AN, antenna

inspection of the first principal component against log(cs) (Fig. 5) confirmed the validity of this categorization.

In the Procrustes ANOVA including all individuals, the interactions between log(cs) and treatment, between log(cs) and morph, and between treatment and morph were all significant (Table 2). In major and minor males, *ser* knockdown affected horn shape (significant main effect of treatment), but not horn shape allometry (non-significant interactions between log(cs) and treatment) (Table 2). In contrast, the treatment of intermediate males did seem to affect horn shape allometry ($F_{1,17} = 2.43$, $P = 0.041$; Table 2). However, because the vector correlation between the allometric vectors of intermediate Ctrl and ser^{RNAi} males was remarkably high (vector correlation = 0.96, vector angle = 15.49°, $P < 0.0001$; Fig. S2), and the ser^{RNAi} group consisted of only 5 individuals, this difference was probably of minor biological relevance and more likely represented a statistical sampling artifact.

The effect of *ser* downregulation, assessed after controlling for allometry, is shown in Fig. 6. In minor and intermediate individuals, ser^{RNAi} causes horns to become straighter and situated onto a narrower base, while in major males it causes horns to become more arched. PCAs of allometry-adjusted coordinates showed comparable results (Fig. S3). In all morphs, Procrustes distances between control and ser^{RNAi} individuals (minor, 0.074; intermediate, 0.092; major, 0.053) were significant at $P < 0.001$, and discriminant analyses confirmed excellent separation of the treatment groups on the basis of horn shape (Fig. 6).

Discussion

Beetle horns are tremendously diverse in both size and shape across species, sexes, as well as in alternate morphs among individuals of the same species (Balthasar 1963; Emlen et al. 2005a). In the majority of horned species, horns grow either disproportionately faster than overall body size resulting in hyperallometric growth, or in a polyphenic fashion, characterized by a threshold body size separating discrete alternate male morphs (Emlen et al. 2006). In both instances, allometry is a major contributor to intraspecific horn shape variation. Yet relatively little is known about the developmental-genetic mechanisms that regulate horn shape in general and its developmental plasticity in particular.

Here, we sought to start exploring the role of Notch signaling in the specification of horn shape in one species, the bull-headed dung beetle *O. taurus*. We focused on Notch signaling because of its well-established role in instructing the formation of traditional appendages such as legs and antennae, while parallel efforts have identified other appendage patterning genes as critical for establishing proximo-distal polarity and relative sizes of horns (Moczek et al. 2006; Moczek and Rose 2009). Combined, this raised the possibility that Notch signaling may have been similarly recruited into the formation of horns. Furthermore, Notch signaling plays an especially critical role in the formation of joints between appendage segment boundaries via the induction of cell death, cell constriction, and cell reorientation—processes that at least in principle could also contribute to the specification

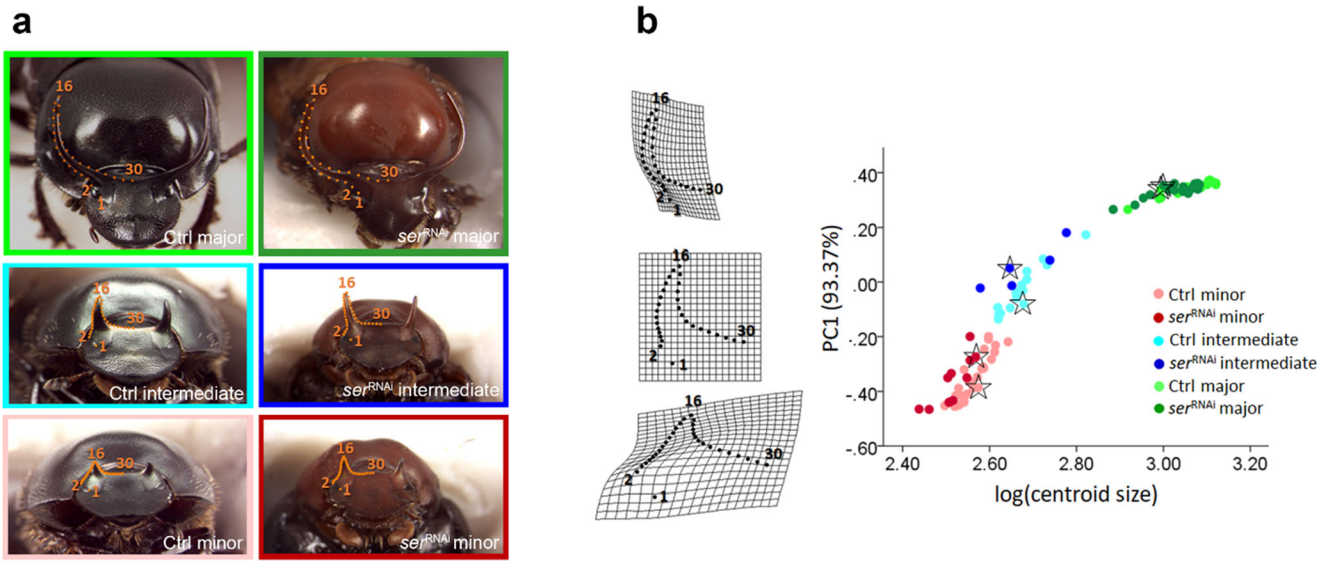

Fig. 5 **a** 2D landmark configuration used to analyze horn shape. Individuals are color-coded based on morph and treatment (ser^{RNAi}, individuals injected with dsRNA, so as to downregulate *serrate* expression; Crtl, control individuals, injected with buffer solution). Landmarks 1, 2, 16, and 30 were homologous in all individuals. The remaining landmarks 3–15 and 17–29 were used to describe curvature and treated as sliding semilandmarks. **b** In the scatterplot, the first principal component of horn shape variation (PC1, accounting for more than 93% of the overall shape variance in the sample) is plotted against the logarithm of horn centroid size, showing a tight relationship between the two variables, i.e., a substantial contribution of allometry to overall horn shape variation. The deformation described by PC1 is shown along the *Y*-axis by means of deformation grids, and depicts the transition between the horn of a minor (PC1 = − 0.46) and that of a major individual (PC1 = 0.37), with intermediate males clustered around PC1 = 0.00. The landmarks shown in the deformation grids correspond in a one-to-one manner to those reported in **a**. The individuals identified with stars in the scatterplot are those pictured in **a**

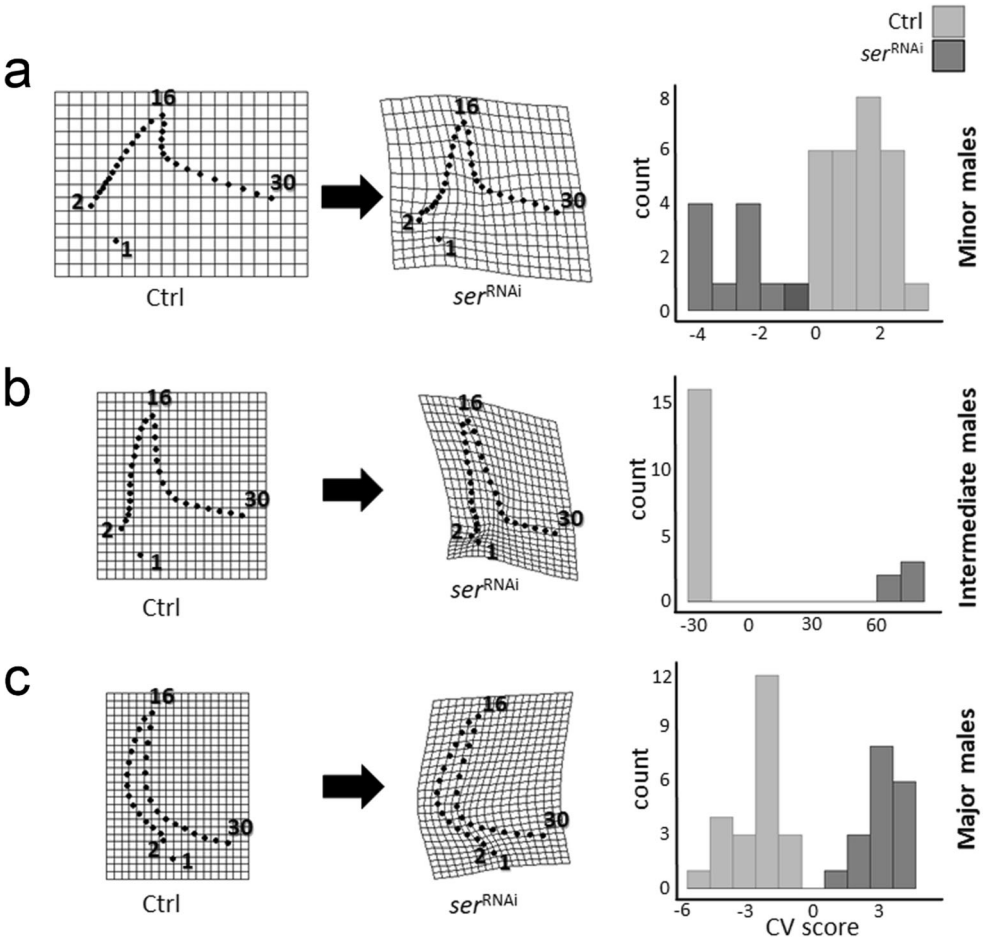

Fig. 6 Horn shape deformation following downregulation of *ser* in each morph. In minor (**a**) and intermediate males (**b**), knockdown of *serrate* causes horns to become straighter and positioned onto a narrower base, while in major males (**c**), the same treatment causes horns to become more arched. Within each morph, the deformation following ser^{RNAi} (second column) is shown alongside the mean shape of buffer-injected (Ctrl) individuals (first column), and is magnified 3× for easier visualization. The histograms (third column) show the distribution of the specimens according to their scores on the discriminant function (CV score). Overall classification accuracy was 97.44% in minor males, and 100% in intermediate and major males, confirming excellent shape differentiation between treatment groups in all morphs. Analyses were performed on allometry-adjusted shape coordinates as described in the "Methods"

of horn shape even though horns do not possess joints (Kijimoto et al. 2010).

We chose *O. taurus* because it affords the opportunity to assess the patterning of horn shape within the same species, yet across distinct morphs, and a wide range of horn sizes. We find that, as in other insects, Notch signaling plays a critical role in patterning diverse appendages such as legs, antennae, and mouthparts—in particular with respect to the formation of joints. Most importantly, we find that Notch signaling also moderately but consistently affects horn shape even after controlling for overall size, yet does so differently for the horns of minor, intermediate, and major males. Taken together, these results suggest that the function of Notch signaling during head horn formation may vary in a complex manner across alternative morphs. Below we discuss the most important implications of our results.

Notch signaling affects horn shape differently for different horn sizes

Previous work has identified diverse appendage patterning genes as being critically required for the proper development of horns, such as the leg gap genes *Dll* and *hth*, or members of the wingless and dpp signaling pathways (Moczek et al. 2006; Moczek and Rose 2009; Wasik and Moczek 2011, 2012). However, experimental perturbations of these pathways typically eliminate or drastically reduce horn formation, making an analysis of their potential involvement in the regulation of horn shape difficult. In contrast, in this study N^{RNAi} and ser^{RNAi}, while resulting in major effects during regular appendage formation, nevertheless yielded in the surviving individuals the expression of the whole range of horn sizes usually present in natural populations. This allowed us to assess the potential significance of Notch signaling for establishing the horn shapes specific for any given horn size. We find that overall ser^{RNAi} had moderate yet reliably detectable effects on horn shape specific to minor and intermediate males in one way, and major males in another way. Specifically, in minor and intermediate males, ser^{RNAi} causes horns to become straighter and form a narrower base. In contrast, in major males, ser^{RNAi} causes horns to become relatively more arched. This raises the possibility that Notch signaling may be operating differently in minor/intermediate and major males, for example, via the activation and inhibition of different target genes, or by interacting with other pathways

operating in specific morphs, paralleling recent finding for the hedgehog-, insulin-, and doublesex-pathways (Kijimoto and Moczek 2016; Ledón-Rettig et al. 2017; Casasa and Moczek 2018), whose horn patterning functions are either limited to or otherwise qualitatively different across major and minor morphs.

Alternatively, Notch signaling may be functioning in essentially the same way across morphs, yet may be contributing to different kinds of shape components by virtue of operating in horns of diverse lengths and diameters. For example, Notch signaling has been studied in detail during the formation of leg joints in *Drosophila*, where it plays a critical role in the contraction, reorientation, and death of cells critical to the establishment of the ball and socket joint during the pupal stage (Suzanne 2016; Kojima 2017). Similar mechanisms may also underlie the specification of horn shape. In fact, moderate cell death is indeed detectable in *O. taurus* head horns during the early pupal stage (Kijimoto et al. 2010). It is conceivable that localized changes in cell death operating in small versus larger horns may be sufficient to bring about the alternate ser^{RNAi}-mediated changes in horn shape detected here. Further studies are needed to detect whether knockdown of Notch signaling affects the spatio-temporal distribution of cell death in different horn size classes. Lastly, we presently cannot fully exclude the possibility that the reduction of limbs mediated by Notch signaling might also influence horn shape indirectly, by freeing up resources for horn development. However, the extent to which horn shape might be influenced by increased resource availability is currently unknown.

Conclusions and future directions

The horns of scarab beetles are a classic example of a morphological evolutionary novelty, which ever since its emergence has undergone one of the most spectacular diversifications in the animal kingdom (Emlen et al. 2005a; Moczek 2005). This study identifies Notch signaling as a contributing regulator of polyphenism in one species famous for its dramatic diversity of horn sizes and shapes across males. It remains unclear, however, whether Notch signaling or other pathways also contribute to variation in horn shape among species, necessitating more comparative studies in the future. Our results also underscore the potential value of examining genes and pathways whose experimental perturbation does not ablate or dramatically reduce focal structures, for understanding other dimensions in the developmental evolution of novel traits, such as the specification and diversification of shape. Lastly, our study highlights the power of integrating functional genetic and geometric morphometric approaches in analyzing subtle but nevertheless biologically important phenotypes in the face of significant allometric variation.

Acknowledgments We would like to thank Kayla Copper, Madison Gits, and Trevor Edgerton for beetle care.

Authors' contributions APM and YH designed the research; JRC and YH performed the research; JRC, ALMM, APM, PTR, and YH analyzed the data and wrote the paper.

Funding information Funding for this study was provided by the National Science Foundation grants (IOS 1256689 and 1901680) as well as a grant from the John Templeton Foundation to APM.

Compliance with ethical standards

Conflict of interest The authors declare that they have no conflict of interest.

References

Adams DC (2004) Character displacement via aggressive interference in Appalachian salamanders. Ecology 85:2664–2670. https://doi.org/10.1890/04-0648

Adams DC, Collyer ML, Kaliontzopoulou A (2019) Geometric morphometric analyses of 2D/3D landmark data

Adams DC, Rohlf FJ, Slice DE (2004) Geometric morphometrics: ten years of progress following the 'revolution.' Italian Journal of Zoology 71:5–16. https://doi.org/10.1080/11250000409356545

Angelini DR, Smith FW, Jockusch EL (2012) Extent with modification: leg patterning in the beetle Tribolium castaneum and the evolution of serial homologs. G3: Genes, Genomes, Genetics 2:235–248. https://doi.org/10.1534/g3.111.001537

Balthasar V (1963) Monographie der Scarabaeidae und Aphodiidae der palaearktischen und orientalischen Region (Coleoptera: Lamellicornia). Tschechoslowakische Akademie der Wissenschaften, Prague

Bishop SA, Klein T, Arias AM, Couso JP (1999) Composite signalling from Serrate and Delta establishes leg segments in Drosophila through Notch. Development 126:2993–3003

Bookstein FL (1991) Morphometric tools for landmark data: geometry and biology. Cambridge University Press, Cambridge

Casasa S, Moczek AP (2019) Evolution of, and via, developmental plasticity: insights through the study of scaling relationships. Integr Comp Biol icz086:. https://doi.org/10.1093/icb/icz086

Casasa S, Moczek AP (2018) Insulin signalling's role in mediating tissue-specific nutritional plasticity and robustness in the horn-polyphenic beetle Onthophagus taurus. Proc R Soc B Biol Sci 285:20181631. https://doi.org/10.1098/rspb.2018.1631

de Celis JF, Garcia-Bellido A, Bray SJ (1996) Activation and function of Notch at the dorsal-ventral boundary of the wing imaginal disc. Development 122:359–369

de Celis JF, Tyler DM, de Celis J, Bray SJ (1998) Notch signalling mediates segmentation of the Drosophila leg. Development 125:4617–4626

Choi HMT, Schwarzkopf M, Fornace ME, et al (2018) Third-generation in situ hybridization chain reaction: multiplexed, quantitative, sensitive, versatile, robust. Development 145:dev165753. https://doi.org/10.1242/dev.165753

Choi J-H, Kijimoto T, Snell-Rood E, Tae H, Yang Y, Moczek AP, Andrews J (2010) Gene discovery in the horned beetle Onthophagus taurus. BMC Genomics 11:703. https://doi.org/10.1186/1471-2164-11-703

Clark-Hachtel CM, Linz DM, Tomoyasu Y (2013) Insights into insect wing origin provided by functional analysis of vestigial in the red

flour beetle, Tribolium castaneum. Proc Natl Acad Sci U S A 110: 16951–16956. https://doi.org/10.1073/pnas.1304332110

Collyer ML, Adams DC (2018) RRPP: An r package for fitting linear models to high-dimensional data using residual randomization. Methods Ecol Evol 9:1772–1779. https://doi.org/10.1111/2041-210X.13029

Collyer ML, Adams DC (2019) RRPP: linear model evaluation with randomized residuals in a permutation procedure

Domínguez M, de Celis JF (1998) A dorsal/ventral boundary established by Notch controls growth and polarity in the Drosophila eye. Nature 396:276–278. https://doi.org/10.1038/24402

Emlen DJ, Hunt J, Simmons LW (2005a) Evolution of sexual dimorphism and male dimorphism in the expression of beetle horns: phylogenetic evidence for modularity, evolutionary lability, and constraint. Am Nat 166(Suppl 4):S42–S68. https://doi.org/10.1086/444599

Emlen DJ, Lavine LC, Ewen-Campen B (2007) On the origin and evolutionary diversification of beetle horns. PNAS 104:8661–8668. https://doi.org/10.1073/pnas.0701209104

Emlen DJ, Marangelo J, Ball B, Cunningham CW (2005b) Diversity in the weapons of sexual selection: horn evolution in the beetle genus Onthophagus (Coleoptera: Scarabaeidae). Evolution 59:1060–1084

Emlen DJ, Szafran Q, Corley LS, Dworkin I (2006) Insulin signaling and limb-patterning: candidate pathways for the origin and evolutionary diversification of beetle 'horns.' Heredity 97:179. https://doi.org/10.1038/sj.hdy.6800868

Goczał J, Rossa R, Tofilski A (2019) Intersexual and intrasexual patterns of horn size and shape variation in the European rhinoceros beetle: quantifying the shape of weapons. Biol J Linn Soc 127:34–43. https://doi.org/10.1093/biolinnean/blz026

Gokhale RH, Shingleton AW (2015) Size control: the developmental physiology of body and organ size regulation. Wiley Interdiscip Rev Dev Biol 4:335–356. https://doi.org/10.1002/wdev.181

Goodall C (1991) Procrustes methods in the statistical analysis of shape. J R Stat Soc Ser B Methodol 53:285–321. https://doi.org/10.1111/j.2517-6161.1991.tb01825.x

Head JJ, Polly PD (2015) Evolution of the snake body form reveals homoplasy in amniote *Hox* gene function. Nature 520:86–89. https://doi.org/10.1038/nature14042

Huxley JS (1932) Problems of relative growth. Methuen and Co., Ltd., London

Kijimoto T, Andrews J, Moczek AP (2010) Programed cell death shapes the expression of horns within and between species of horned beetles. Evolution & Development 12:449–458. https://doi.org/10.1111/j.1525-142X.2010.00431.x

Kijimoto T, Costello J, Tang Z, Moczek AP, Andrews J (2009) EST and microarray analysis of horn development in Onthophagus beetles. BMC Genomics 10:504. https://doi.org/10.1186/1471-2164-10-504

Kijimoto T, Moczek AP (2016) Hedgehog signaling enables nutrition-responsive inhibition of an alternative morph in a polyphenic beetle. Proc Natl Acad Sci 113:5982–5987. https://doi.org/10.1073/pnas.1601505113

Klingenberg CP (2016) Size, shape, and form: concepts of allometry in geometric morphometrics. Dev Genes Evol 226:113–137. https://doi.org/10.1007/s00427-016-0539-2

Kodric-Brown A, Sibly RM, Brown JH (2006) The allometry of ornaments and weapons. PNAS 103:8733–8738. https://doi.org/10.1073/pnas.0602994103

Kojima T (2004) The mechanism of Drosophila leg development along the proximodistal axis. Develop Growth Differ 46:115–129. https://doi.org/10.1111/j.1440-169X.2004.00735.x

Kojima T (2017) Developmental mechanism of the tarsus in insect legs. Current Opinion in Insect Science 19:36–42. https://doi.org/10.1016/j.cois.2016.11.002

Koyama T, Mendes CC, Mirth CK (2013) Mechanisms regulating nutrition-dependent developmental plasticity through organ-specific effects in insects. Front Physiol 4:263. https://doi.org/10.3389/fphys.2013.00263

Ledón-Rettig CC, Zattara EE, Moczek AP (2017) Asymmetric interactions between *doublesex* and tissue- and sex-specific target genes mediate sexual dimorphism in beetles. Nat Commun 8:14593. https://doi.org/10.1038/ncomms14593

Linz DM, Hu Y, Moczek AP (2019) The origins of novelty from within the confines of homology: the developmental evolution of the digging tibia of dung beetles. Proc R Soc B Biol Sci 286:20182427. https://doi.org/10.1098/rspb.2018.2427

Liu W (2013) Bmdelta phenotype implies involvement of Notch signaling in body segmentation and appendage development of silkworm, Bombyx mori. Arthropod Struct Dev 42:143–151. https://doi.org/10.1016/j.asd.2012.10.002

Macagno ALM, Moczek AP, Pizzo A (2016) Rapid divergence of nesting depth and digging appendages among tunneling dung beetle populations and species. Am Nat 187:E143–E151. https://doi.org/10.1086/685776

Macagno ALM, Zattara EE, Ezeakudo O et al (2018) Adaptive maternal behavioral plasticity and developmental programming mitigate the transgenerational effects of temperature in dung beetles. Oikos 127: 1319–1329. https://doi.org/10.1111/oik.05215

McCullough EL, Tobalske BW, Emlen DJ (2014) Structural adaptations to diverse fighting styles in sexually selected weapons. PNAS 111: 14484–14488. https://doi.org/10.1073/pnas.1409585111

Mito T, Shinmyo Y, Kurita K, Nakamura T, Ohuchi H, Noji S (2011) Ancestral functions of Delta/Notch signaling in the formation of body and leg segments in the cricket Gryllus bimaculatus. Development 138:3823–3833. https://doi.org/10.1242/dev.060681

Mitteroecker P, Gunz P (2009) Advances in geometric morphometrics. Evol Biol 36:235–247. https://doi.org/10.1007/s11692-009-9055-x

Mitteroecker P, Gunz P, Bernhard M, Schaefer K, Bookstein FL (2004) Comparison of cranial ontogenetic trajectories among great apes and humans. J Hum Evol 46:679–698. https://doi.org/10.1016/j.jhevol.2004.03.006

Mitteroecker P, Gunz P, Windhager S, Schaefer K (2013) A brief review of shape, form, and allometry in geometric morphometrics, with applications to human facial morphology. Hystrix It J Mamm 24: 59–66. https://doi.org/10.4404/hystrix-24.1-6369

Moczek AP (2005) The evolution and development of novel traits, or how beetles got their horns. BioScience 55:937–951. https://doi.org/10.1641/0006-3568(2005)055[0937:TEADON]2.0.CO;2

Moczek AP, Emlen DJ (1999) Proximate determination of male horn dimorphism in the beetle Onthophagus taurus (Coleoptera: Scarabaeidae). J Evol Biol 12:27–37. https://doi.org/10.1046/j.1420-9101.1999.00004.x

Moczek AP, Rose D, Sewell W, Kesselring BR (2006) Conservation, innovation, and the evolution of horned beetle diversity. Dev Genes Evol 216:655–665

Moczek AP, Rose DJ (2009) Differential recruitment of limb patterning genes during development and diversification of beetle horns. PNAS 106:8992–8997. https://doi.org/10.1073/pnas.0809668106

Müller GB, Wagner GP (1991) Novelty in evolution: restructuring the concept. Annu Rev Ecol Syst 22:229–256. https://doi.org/10.1146/annurev.es.22.110191.001305

Nijhout HF, Riddiford LM, Mirth C, Shingleton AW, Suzuki Y, Callier V (2014) The developmental control of size in insects. Wiley Interdiscip Rev Dev Biol 3:113–134. https://doi.org/10.1002/wdev.124

O'Brien DM, Allen CE, Van Kleeck MJ et al (2018) On the evolution of extreme structures: static scaling and the function of sexually selected signals. Anim Behav 144:95–108. https://doi.org/10.1016/j.anbehav.2018.08.005

Outomuro D, Johansson F (2017) A potential pitfall in studies of biological shape: does size matter? J Anim Ecol 86:1447–1457. **https://doi.org/10.1111/1365-2656.12732**

Pitchers W, Pool JE, Dworkin I (2013) Altitudinal clinal variation in wing size and shape in African Drosophila melanogaster: one cline or many? Evolution 67:438–452. **https://doi.org/10.1111/j.1558-5646.2012.01774.x**

Pitchers W, Pool JE, Dworkin I (2013) Altitudinal clinal variation in wing size and shape in African Drosophila melanogaster: one cline or many? Evolution 67:438–452. **https://doi.org/10.1111/j.1558-5646.2012.01774.x**

Prpic N-M, Damen WGM (2009) Notch-mediated segmentation of the appendages is a molecular phylotypic trait of the arthropods. Dev Biol 326:262–271. **https://doi.org/10.1016/j.ydbio.2008.10.049**

Prpic N-M, Posnien N (2016) Size and shape—integration of morphometrics, mathematical modelling, developmental and evolutionary biology. Dev Genes Evol 226:109–112. **https://doi.org/10.1007/s00427-016-0536-5**

R Core Team (2018) R: a language and environment for statistical computing. R Foundation for Statistical Computing, Vienna, Austria

Rauskolb C, Irvine KD (1999) Notch-mediated segmentation and growth control of the Drosophila leg. Dev Biol 210:339–350. **https://doi.org/10.1006/dbio.1999.9273**

Rohlf FJ (2015) The tps series of software. Hystrix It J Mamm 26:9–12

Rohlf FJ. 2017a. tpsRelw32. Stony Brook: Department of Ecology and Evolution, State University of New York. **Available at** http://life.bio.sunysb.edu/morph/

Rohlf FJ. 2017b. tpsSmallw32. Stony Brook: Department of Ecology and Evolution, State University of New York. **Available at** http://life.bio.sunysb.edu/morph/

Rohlf FJ. 2018a. tpsDig2w32. Stony Brook: Department of Ecology and Evolution, State University of New York. **Available at** http://life.bio.sunysb.edu/morph/

Rohlf FJ. 2018b. tpsUtil32. Stony Brook: Department of Ecology and Evolution, State University of New York. **Available at** http://life.bio.sunysb.edu/morph/

Rohner PT, Roy J, Schäfer MA et al (2019) Does thermal plasticity align with local adaptation? An interspecific comparison of wing morphology in sepsid flies. J Evol Biol 32:463–475. **https://doi.org/10.1111/jeb.13429**

Romiti F, Redolfi De Zan L, Piras P, Carpaneto GM (2017) Shape variation of mandible and head in Lucanus cervus (Coleoptera: Lucanidae): a comparison of morphometric approaches. Biol J Linn Soc 120:836–851. **https://doi.org/10.1093/biolinnean/blw001**

Schäfer MA, Berger D, Rohner PT et al (2018) Geographic clines in wing morphology relate to colonization history in New World but not Old World populations of yellow dung flies. Evolution 72:1629–1644. **https://doi.org/10.1111/evo.13517**

Schlager S (2017) Chapter 9 Morpho and Rvcg – shape analysis in R: R-packages for geometric morphometrics, shape analysis and surface manipulations. In: Zheng G, Li S, Székely G (eds) Statistical shape and deformation analysis. Academic Press, pp 217–256

Schneider CA, Rasband WS, Eliceiri KW (2012) NIH Image to ImageJ: 25 years of image analysis. Nat Methods 9:671–675

Shafiei M, Moczek AP, Nijhout HF (2001) Food availability controls the onset of metamorphosis in the dung beetle Onthophagus taurus (Coleoptera: Scarabaeidae). Physiol Entomol 26:173–180. **https://doi.org/10.1046/j.1365-3032.2001.00231.x**

Simmons LW, Fitzpatrick JL (2016) Sperm competition and the coevolution of pre- and postcopulatory traits: weapons evolve faster than testes among onthophagine dung beetles. Evolution 70:998–1008. **https://doi.org/10.1111/evo.12915**

Suzanne M (2016) Molecular and cellular mechanisms involved in leg joint morphogenesis. Semin Cell Dev Biol 55:131–138. **https://doi.org/10.1016/j.semcdb.2016.01.032**

Testa ND, Dworkin I (2016) The sex-limited effects of mutations in the EGFR and TGF-β signaling pathways on shape and size sexual dimorphism and allometry in the Drosophila wing. Dev Genes Evol 226:159–171. **https://doi.org/10.1007/s00427-016-0534-7**

Thompson DAW (1917) On growth and form. Cambridge University Press, Cambridge

Tomkins JL, Kotiaho JS, LeBas NR (2005) Matters of scale: positive allometry and the evolution of male dimorphisms. Am Nat 165:389–402. **https://doi.org/10.1086/427732**

Wasik BR, Moczek AP (2011) Decapentaplegic (dpp) regulates the growth of a morphological novelty, beetle horns. Dev Genes Evol 221:17–27. **https://doi.org/10.1007/s00427-011-0355-7**

Wasik BR, Moczek AP (2012) Pangolin expression influences the development of a morphological novelty: beetle horns. Genesis 50:404–414. **https://doi.org/10.1002/dvg.20814**

Zelditch ML, Swiderski DL, Sheets HD, Fink WL (2004) Geometric morphometrics for biologists: a primer, 1st edn. Academic Press, London